J|A|C|S
ARTICLES

Published on Web 04/29/2010

A Single Watson−Crick G·C Base Pair in Water: Aqueous Hydrogen Bonds in Hydrophobic Cavities

Tomohisa Sawada[†] and Makoto Fujita*[,†,‡]

Department of Applied Chemistry, School of Engineering, The University of Tokyo, and CREST (JST), 7-3-1 Hongo, Bunkyo-ku, Tokyo 113-8656, Japan

Received March 6, 2010; E-mail: mfujita@appchem.t.u-tokyo.ac.jp

Abstract: Hydrogen bond (H-bond) formation in water has been a challenging task because water molecules are constant competitors. In biological systems, however, stable H-bonds are formed by shielding the H-bonding sites from the competing water molecules within hydrophobic pockets. Inspired by the nature's elaborated way, we found that even mononucleotides (G and C) can form the minimal G·C Watson−Crick pair in water by simply providing a synthetic cavity that efficiently shields the Watson−Crick H-bonding sites. The minimal Watson−Crick structure in water was elucidated by NMR study and firmly characterized by crystallographic analysis. The crystal structure also displays that, within the cavity, coencapsulated anions and solvents efficiently mediate the minimal G·C Watson−Crick pair formation. Furthermore, the competition experiments with the other nucleobases clearly revealed the evident selectivity for the G·C base pairing in water. These results show the fact that a H-bonded nucleobase pair was effectively induced and stabilized in the local environment of an artificial hydrophobic cavity.

Introduction

Hydrogen bonds play a pivotal role in a vast number of biological processes ranging from establishing structural motifs to governing enzyme catalysis.[1] In aqueous environments, however, water molecules are constant competitors. Even the impressive fidelity of the three hydrogen bonds in a single Watson−Crick G·C nucleobase pair is insufficient to pay the cost of assembly and hydrogen bonds between individual nucleotides or nucleobases are not observed in aqueous solution until higher order oligomers are used ($n \geq 4$).[2] Accordingly, a majority of studies involving hydrogen bonds, which are extensive,[3] typically employ noncompetitive organic solvents. Several artificial hydrogen bonded systems have judiciously exploited extended hydrogen bond motifs,[4] additional weak interactions (aromatic stacking,[5] or the hydrophobic effect[6,7]) to help cover the energetic costs of breaking hydrogen bonds formed with water molecules and can assemble in aqueous media.

In biological systems, recognition sites involving hydrogen bonds are shielded from the competing water molecules within hydrophobic microenvironments such as those found within the cell membranes, proteins pockets,[8] or the aromatic stacks within the DNA helix[2a] or G-quartets.[9] In the mid-1990s, Nowick and co-workers reported that the hydrogen bond directed recognition of adenine derivatives occurred within the shielding environment of micelles in aqueous solution.[10] Similar work by Komiyama and co-workers showed that the artificial hydrogen bond receptors within the microenvironment of polymers adsorbed nucleobases and derivatives from aqueous solutions.[11]

Recently, we reported a new strategy for achieving the pairwise recognition of single and double nucleobase pairs in

[†] The University of Tokyo.
[‡] CREST (JST).

(1) Jeffrey, G. A.; Saenger, W. *Hydrogen Bonding in Biological Structures*; Springer: Berlin, 1991.
(2) (a) Saenger, W. *Principles of Nucleic Acid Structure*; Springer: New York, 1984. (b) Philp, D.; Stoddart, J. F. *Angew. Chem., Int. Ed. Engl.* **1996**, *35*, 1154–1196.
(3) (a) Prins, L. J.; Reinhoudt, D. N.; Timmerman, P. *Angew. Chem., Int. Ed.* **2001**, *40*, 2382–2426. (b) Jeffrey, G. A. *An Introduction to Hydrogen Bonding*; Oxford University Press, New York, 1997.
(4) (a) Fenniri, H.; Mathivanan, P.; Vidale, K. L.; Sherman, D. M.; Hallenga, K.; Wood, K. V.; Stowell, J. G. *J. Am. Chem. Soc.* **2001**, *123*, 3854–3855. (b) Fenniri, H.; Deng, B.-L.; Ribbe, A. E. *J. Am. Chem. Soc.* **2002**, *124*, 11064–11072. (c) Johnson, R. S.; Yamazaki, T.; Kovalenko, A.; Fenniri, H. *J. Am. Chem. Soc.* **2007**, *129*, 5735–5743. (d) Rzepecki, P.; Hochdörffer, K.; Schaller, T.; Zienau, J.; Harms, K.; Ochsenfeld, C.; Xie, X.; Schrader, T. *J. Am. Chem. Soc.* **2008**, *130*, 586–591.
(5) (a) Rotello, V. M.; Viani, E. A.; Deslongchamps, G.; Murray, B. A.; Rebek, J., Jr. *J. Am. Chem. Soc.* **1993**, *115*, 797–798. (b) Kato, Y.; Conn, M. M.; Rebek, J., Jr. *J. Am. Chem. Soc.* **1994**, *116*, 3279–3284. (c) Kato, Y.; Conn, M. M.; Rebek, J., Jr. *Proc. Natl. Acad. Sci. U.S.A.* **1995**, *92*, 1208–1212.
(6) (a) Constant, J. F.; Laûgaa, P.; Roques, B. P.; Lhomme, J. *Biochemisty* **1988**, *27*, 3997–4003. (b) Jourdan, M.; Garcia, J.; Lhomme, J.; Teulade-Fichou, M.-P.; Vigneron, J.-P.; Lehn, J.-M. *Biochemistry* **1999**, *38*, 14205–14213.
(7) (a) Hirschberg, J. H. K. K.; Brunsveld, L.; Ramzl, A.; Vekemans, J. A. J. M.; Sijbesma, R. P.; Meijer, E. W. *Nature* **2000**, *407*, 167–170. (b) Brunsveld, L.; Vekemans, J. A. J. M.; Hirschberg, J. H. K. K.; Sijbesma, R. P.; Meijer, E. W. *Proc. Natl. Acad. Sci. U.S.A.* **2002**, *99*, 4977–4982.
(8) (a) Branden, C.; Tooze, J. *Introduction to Protein Structure*; Garland Pub.: New York, 1999. (b) Petsko, G. A.; Ringe, D. *Protein Structure and Function*; New Science Press: London, 2004.
(9) (a) Sen, D.; Gilbert, W. *Curr. Opin. Struct. Biol.* **1991**, *1*, 435–438. (b) Williamson, J. R. *Curr. Opin. Struct. Biol.* **1993**, *3*, 357–362. (c) Davis, J. T. *Angew. Chem., Int. Ed.* **2004**, *43*, 668–698.
(10) (a) Nowick, J. S.; Chen, J. S. *J. Am. Chem. Soc.* **1992**, *114*, 1107–1108. (b) Nowick, J. S.; Chen, J. S.; Noronha, G. *J. Am. Chem. Soc.* **1993**, *115*, 7636–7644.
(11) (a) Asanuma, H.; Hishiya, T.; Komiyama, M. *Chem. Lett.* **1998**, 1087–1088. (b) Asanuma, H.; Ban, T.; Gotoh, S.; Hishiya, T.; Komiyama, M. *Macromolecules* **1998**, *31*, 371–377.

10.1021/ja101718c

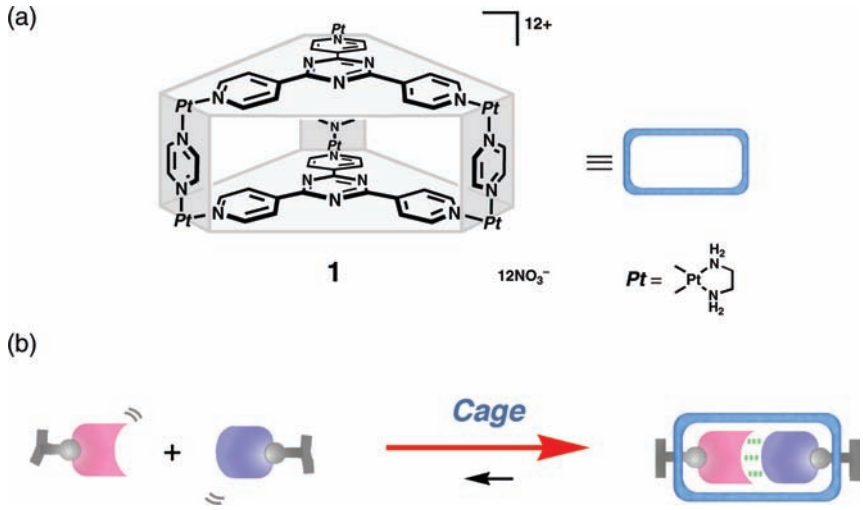

Figure 1. (a) Structure of cage **1**. (b) Schematic representation for the base pair formation in the cavity of **1**.

water.[12] Self-assembled coordination cages with pyrazine pillars (**1** in Figure 1a) provide a flat, hydrophobic microenvironment with an ideal interplanary distance (∼6.6 Å) for the binding of single planar aromatic molecules.[13] In this new strategy, illustrated in Figure 1b, cage **1** encapsulates the planar nucleobases, shields the nucleobase hydrogen bonding motifs from the surrounding water molecules, and facilitates the aqueous formation of minimal nucleobase pairs. Single mononucleotides A and U formed reversed (anti-) Hoogsteen type A·U base pair and dinucleosides AA and TT monophosphates formed reversed Hoogsteen type stacked duplexes. X-ray crystallography afforded final structural proof of the isolated single and double nucleobase pairs. The high proclivity of coordination cages to afford X-ray quality single crystals is a particular advantage given the importance of X-ray crystallography in obtaining detailed structural information of nucleic acids.[14] However, the crystallographic investigation of nucleic acids remains hindered by the difficulty in growing crystals and subsequently obtaining high quality data. Thus, our new strategy not only provides a suitable microenvironment for hosting hydrogen bonds in aqueous solution, but also establishes a new method for obtaining detailed structural information of nucleobase pairs.

We now report the formation of a single Watson−Crick G·C base pair in aqueous solution case and detail specific interactions of anions and water molecules with the isolated base pairs observed by X-ray crystallography. Solution state NMR studies and competition experiments emphasize the selectivity and robustness of the G·C hydrogen bonding motif.

Results

Encapsulation of a G·C Base Pair in Water. Stirring an aqueous solution of disodium 5′-guanosine monophosphate **2a** (2 μmol) and disodium 5′-cytidine monophosphate **3a** (2 μmol) in the presence of cage **1** (2 μmol) resulted in the formation of host−guest complex of **1**⊃(**2a**·**3a**), as evidenced by ^{1}H NMR (Figure 2). The nucleobase protons of **2a** and **3a** were shifted upfield ($\Delta\delta$ = 0.55 for G8 of guanosine **2a**; 0.48 and 0.60 for C5 and C6 of cytidine **3a**) due to shielding from the aromatic triazine panels after encapsulation.[15] The nearby ribose 1′ protons of **2a** (G1′) and **3a** (C1′) were also shielded and shifted upfield ($\Delta\delta$ = 0.79 and 0.46, respectively) (Figure 2). The chemical shifts of ribose protons 2′∼5′ of both **2a** and **3a** remain unchanged as they remained further outside the cavity. These observations strongly suggest that the nucleobase moieties reside inside the cavity and shielded by the aromatic panels; whereas the ribose moieties remain outside. The host and guest aromatic signals of **1**⊃(**2a**·**3a**) are considerably broadened and indicate a slow exchange process.

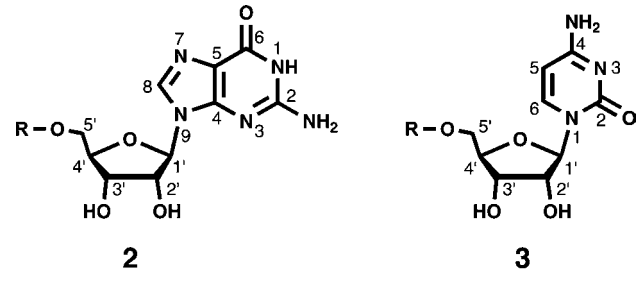

(12) Sawada, T.; Yoshizawa, M.; Sato, S.; Fujita, M. *Nat. Chem.* **2009**, *1*, 53–56.

(13) (a) Kumazawa, K.; Biradha, K.; Kusukawa, T.; Okano, T.; Fujita, M. *Angew. Chem., Int. Ed.* **2003**, *42*, 3909–3913. (b) Yoshizawa, M.; Nakagawa, J.; Kumazawa, K.; Nagao, M.; Kawano, M.; Ozeki, T.; Fujita, M. *Angew. Chem., Int. Ed.* **2005**, *44*, 1810–1813. (c) Yoshizawa, M.; Ono, K.; Kumazawa, K.; Kato, T.; Fujita, M. *J. Am. Chem. Soc.* **2005**, *127*, 10800–10801. (d) Yoshizawa, M.; Kumazawa, K.; Fujita, M. *J. Am. Chem. Soc.* **2005**, *127*, 13456–13457. (e) Ono, K.; Yoshizawa, M.; Kato, T.; Watanabe, K.; Fujita, M. *Angew. Chem., Int. Ed.* **2007**, *46*, 1803–1806. (f) Ono, K.; Yoshizawa, M.; Kato, T.; Fujita, M. *Chem. Commun.* **2008**, 2328–2330. (g) Yamauchi, Y.; Yoshizawa, M.; Fujita, M. *J. Am. Chem. Soc.* **2008**, *130*, 5832–5833. (h) Ono, K.; Yoshizawa, M.; Akita, M.; Kato, T.; Tsunobuchi, Y.; Ohkoshi, S.; Fujita, M. *J. Am. Chem. Soc.* **2009**, *131*, 2782–2783. (i) Ozaki, Y.; Kawano, M.; Fujita, M. *Chem. Commun.* **2009**, 4245–4247. (j) Ono, K.; Klosterman, J. K.; Yoshizawa, M.; Sekiguchi, K.; Tahara, T.; Fujita, M. *J. Am. Chem. Soc.* **2009**, *131*, 12526–12527. (k) Yamauchi, Y.; Yoshizawa, M.; Akita, M.; Fujita, M. *Proc. Natl. Acad. Sci. U.S.A.* **2009**, *106*, 10435–10437. (l) Yamauchi, Y.; Yoshizawa, M.; Akita, M.; Fujita, M. *J. Am. Chem. Soc.* **2010**, *132*, 960–966.

(14) (a) Clowney, L.; Jain, S. C.; Srinivasan, A. R.; Westbrook, J.; Olson, W. K.; Berman, H. M. *J. Am. Chem. Soc.* **1996**, *118*, 509–518. (b) Gelbin, A.; Schneider, B.; Clowney, L.; Hsieh, S.; Olson, W. K.; Berman, H. M. *J. Am. Chem. Soc.* **1996**, *118*, 519–529. (c) Tereshko, V.; Minasov, G.; Egli, M. *J. Am. Chem. Soc.* **1999**, *121*, 3590–3595. (d) Egli, M. *Curr. Opin. Chem. Biol.* **2004**, *8*, 580–591. (e) Egli, M.; Pallna, P. S. *Auun. Rev. Biophys. Biomol. Struct.* **2007**, *36*, 281–305. (f) Mooers, B. H. M. *Methods* **2009**, *47*, 168–176. (g) Salon, J.; Sheng, J.; Gan, J.; Huang, Z. *J. Org. Chem.* **2010**, *75*, 637–641.

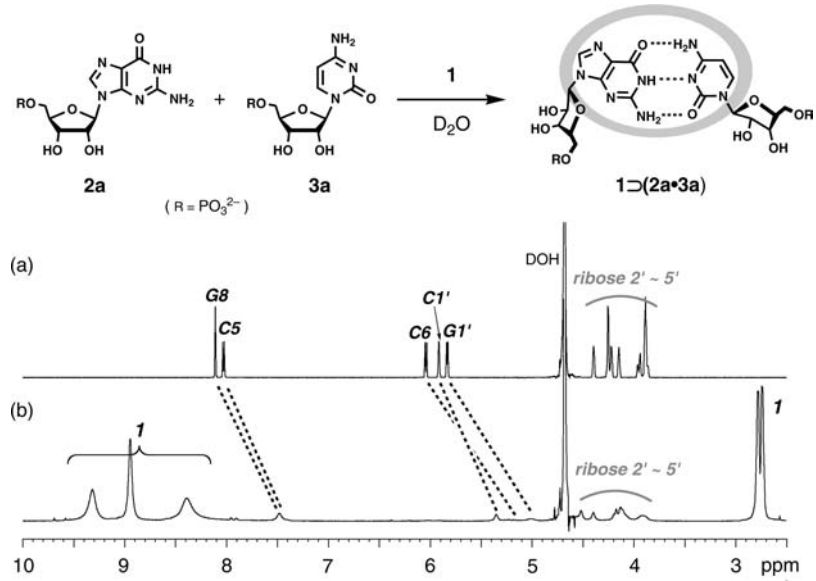

Figure 2. Schematic representation of G·C H-bonding pair formation in water and ^{1}H NMR spectra of (a) **2a** + **3a** and (b) **1**⊃(**2a**·**3a**) encapsulation complex (500 MHz, 300 K) in D_2O.

X-ray Crystallographic Analysis. Final structural proof of the single G·C Watson−Crick base pair was provided by X-ray analysis. Single crystals were obtained by the overnight evaporation of an acetate buffer solution (pH 5.1) of **1′**⊃(**2b**·**3b**) at ambient temperature (where, **1′** is analogous to **1** with *S*,*S*-1,2 diaminocyclohexane instead of ethylenediamine).[16] Cage **1′** not only provides a shielded hydrophobic environment, but yields high quality diffraction data due to the robust crystallinity of the rigid cage framework and the G·C base pair was clearly observed within the cage framework. As a result, the overall structure quality and resolution is quite high and textbook Watson−Crick H-bonds were observed between N1(G)···N3(C), NH_2(G)···O2(C), and O6(G)···NH_2(C) at 2.92, 2.86, and 2.81 Å, respectively (Figure 3). Similar to stacked base pairs in DNA, the G·C base pair stacks with electron-poor triazine panels (∼3.3 Å) and these aromatic−aromatic interactions presumably further stabilize the G·C pair.

The G·C pair cannot fill the entire bay of host **1′** and refinement revealed the coencapsulation of a water molecule and nitrate counterion, both with 100% occupancy (Figure 3a). The nitrate anion (*N*) is located near cytidine **3b** and one nitrate oxygen atom is bound through a hydrogen on the exocyclic cytidine amino group, O2(*N*)···NH_2(C): 2.90 Å, and the second nitrate oxygen interacts through a hydrogen bond with the cytidine C5−H5, O4(*N*)···CH(C): 3.43 Å. This unusual, but favorable, interaction between cytidine and a nitrate anion was recently predicted by a DFT study.[17] Cation−nucleobase interactions are well studied,[18] but disfavored within the cationic framework of host **1**. The interactions of DNA base pairs with anions are relatively unexplored[19] but can also alter the acidities of the nucleobase protons involved in hydrogen bonds and the nucleobase tautomeric equilibria, and are thus important for the better understanding of nucleobase pairing.

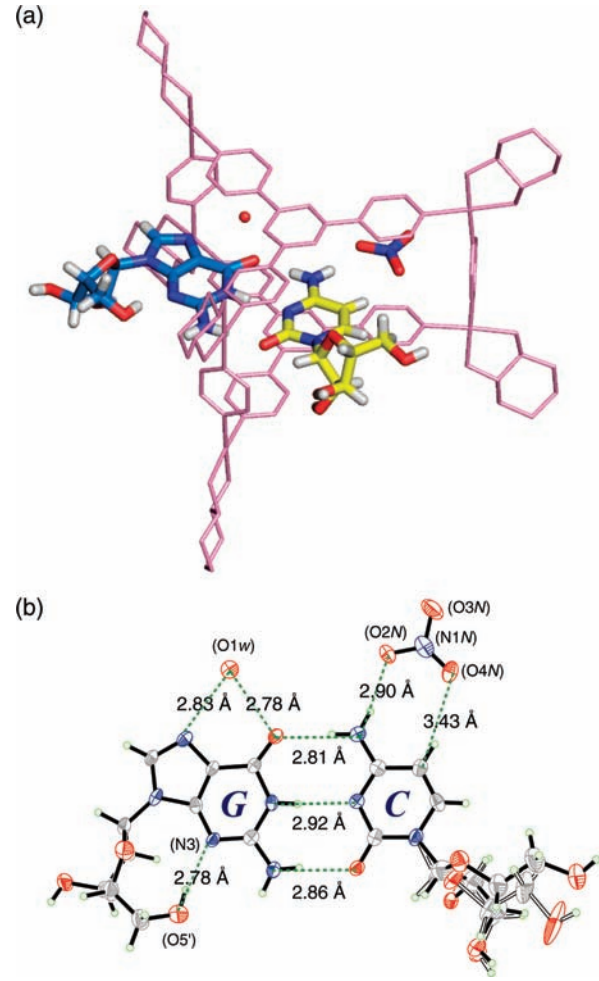

Figure 3. X-ray crystal structure of **1′**⊃(**2b**·**3b**). (a) Overhead view and (b) thermal ellipsoid drawing of base pair part within **1′** (30% probability). Solvent molecules (H_2O) and counteranions (NO_3^-) outside the cavity of **1′** are omitted for clarity.

(15) All signals were assigned from ^{15}N/^{1}H HMBC measurements with ^{15}N-labeled mononucleotides. See Supporting Information for more details.

(16) In cage **1′** the ethylenediamine Pt^{II} complex corners were replaced with *S*,*S*-1,2 diaminocyclohexane Pt^{II} complexes in order to solve false symmetry issues. (See Hatakeyama, Y.; Sawada, T.; Kawano, M.; Fujita, M. *Angew. Chem., Int. Ed.* **2009**, *48*, 8695–8698.) The nucleoside monophosphates were replaced with the nucleoside **2b** and **3b** to facilitate crystallization.

(17) Tehrani, Z. A.; Fattahi, A. *J. Mol. Struct.: THEOCHEM* **2009**, *913*, 277–283.

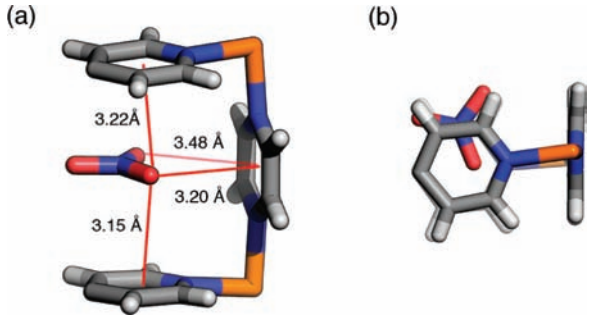

Figure 4. Views of anion−π interactions in the X-ray crystal structure of **1′**⊃(**2b·3b**); (a) Side view with atom−centroid distances indicated and (b) top view illustrating relative positioning. Hydrogens and other selected atoms removed for the sake of clarity.

Confined within the cavity of cage **1**, anion−π interactions between the negatively charged nitrate and the electron poor aromatic cage framework were inevitable. In contrast to cation−π interactions, favorable (16−60 kJ mol^{-1}) anion−π interactions are counterintuitive, synthetically challenging, and less understood.[20] To date, the majority of computational studies focused on interactions involving monatomic anions and only recently have interactions involving more complex multiatomic anions with a dispersed charge, for example, nitrates, been investigated.[21] In the crystal structure of **1′**⊃(**2b·3b**), the nitrate anion that coordinates to the G·C base pair is trapped between the two coordinating pyridines of the electron deficient triazine panels (Figure 4). The nitrate assumed a parallel geometry relative to the planes of the pyridines, which are not perfectly parallel but slightly distorted (∼7°) due to the squeezing of cage **1** onto the G·C pair. Similar to solid-state interactions between nitrate anions and highly π-acidic pyrazine[22] or triazine rings,[21b,c] the nitrate anion interacts with the adjacent π-systems primarily via a single oxygen atom. This nitrate oxygen atom O4(*N*), which also interacts with the cytidine C5−H5, rests between the centroids of the pyridine rings, centroid···O distances are 3.22 and 3.15 Å, but slightly offset (∼0.2 Å). The same oxygen atom also sits above the perpendicular face of the bis-coordinated pyrazine pillar with a centroid···O distance of 3.20 Å. According to calculations at the RI-MP2 level,[23] anion−π interactions are additive and the nearly equidistant positioning of oxygen atom O3(*N*) could indicate a similar additive phenomenon. In the T-geometry relative to the pyrazine, a second oxygen atom of the nitrate, O3(*N*), is also located in close proximity to the pyrazine face, centroid···O distance of 3.48 Å, but is offset ∼38° from the perpendicular axis. Pyridine rings are typically much less π-acidic than triazines, where a majority of anion−π interactions have been observed, but in cage **1**, the pyridines are activated by the pendant central triazine and by coordination to the Pt metal centers. And, although there exist many crystal structures of cage **1** and derivatives[13,24] where nitrates have been almost exclusively used as the counteranion of choice, until now the nitrates have always been found outside of the hydrophobic cavity, typically nearly the metal centers. Only the unique congruence of multiple favorable host−guest and guest−guest interactions presented in **1′**⊃(**2b·3b**) succeeded in inducing a hydrophilic nitrate counterion into the hydrophobic cavity of cage **1**.

The localized water molecule in the crystal structure G·C pair (**2b·3b**) is also noteworthy as the hydration of nucleic acid bases and base pairs directly influences the conformations and properties of DNA molecules and extensive statistical and computational studies have located several binding sites for each nucleobase from DNA decamer X-ray structures.[25] Because of the restrictive cavity size and nearby pyrazine ligand, the single water molecule (*w*) of **1′**⊃(**2b·3b**) is located between the standard W1 and W2 sites of guanosine[25b] and bridges the guanosine N7 and O6 atoms; with O(*w*)···N7 = 2.83 Å and O(*w*)···O6 = 2.78 Å (Figure 5a). Unlike sites W1 and W2, which are derived from hydration within the minor and major grooves of DNA decamers, the water molecule here lies completely in plane with the base-pair, most likely due to the restrictive cavity height.

In contrast, the previously reported Hoogsteen A·U base-pair **1′**⊃(**4·5**) possesses a larger cross-section and more effectively filled cage **1′**. The encapsulation of a nitrate anion is

(18) (a) Lippert, B. *Coord. Chem. Rev.* **1999**, *182*, 263–295. (b) Jamieson, E. R.; Lippard, S. J. *Chem. Rev.* **1999**, *99*, 2467–2498. (c) Lippert, B. *Coord. Chem. Rev.* **2000**, *200−202*, 487–516. (d) Wang, D.; Lippard, S. J. *Nat. Rev. Drug Discovery* **2005**, *4*, 307–320. (e) Clever, G. H.; Kaul, C.; Carell, T. *Angew. Chem., Int. Ed.* **2007**, *46*, 6226–6236. (f) Zeglis, B. M.; Pierre, V. C.; Barton, J. K. *Chem. Commun.* **2007**, 4565–4579.

(19) The limited examples of nucleobase-anion interactions in case of protonated or coordinated nucleobases were reported. See examples of cytosine-nitrate interaction (a) Lippert, B.; Lock, C. J. L.; Speranzini, R. A. *Inorg. Chem.* **1981**, *20*, 335–342. (b) Cherouana, A.; Bouchouit, K.; Bendjeddou, L.; Benali-Cherif, N. *Acta Crystallogr.* **2003**, *E59*, o983–o985.

(20) (a) Mascal, M.; Armstrong, A.; Bartberger, M. D. *J. Am. Chem. Soc.* **2002**, *124*, 6274–6276. (b) Alkorta, I.; Rozas, I.; Elguero, J. *J. Am. Chem. Soc.* **2002**, *124*, 8593–8598. (c) Quiñonero, D.; Garau, C.; Frontera, A.; Ballester, P.; Costa, A.; Deyà, P. M. *Chem. Phys. Lett.* **2002**, *359*, 486–492. (d) Quiñonero, D.; Garau, C.; Rotger, C.; Frontera, A.; Ballester, P.; Costa, A.; Deyà, P. M. *Angew. Chem., Int. Ed.* **2002**, *41*, 3389–3392. (e) Gamez, P.; Mooibroek, T. J.; Teat, S. J.; Reedijk, J. *Acc. Chem. Res.* **2007**, *40*, 435–444. (f) Schottel, B. L.; Chifotides, H. T.; Dunbar, K. R. *Chem. Soc. Rev.* **2008**, *37*, 68–83. (g) Hay, B. P.; Bryantsev, V. S. *Chem. Commun.* **2008**, 2417–2428.

(21) (a) Kim, D.; Tarakeshwar, P.; Kim, K. S. *J. Phys. Chem. A* **2004**, *108*, 1250–1258. (b) Maheswari, P. U.; Modec, B.; Pevec, A.; Kozlevčar, B.; Massera, C.; Gamez, P.; Reedijk, J. *Inorg. Chem.* **2006**, *45*, 6637–6645. (c) Casellas, H.; Massera, C.; Buda, F.; Gamez, P.; Reedijk, J. *New J. Chem.* **2006**, *30*, 1561–1566. (d) Zaccheddu, M.; Filippi, C.; Buda, F. *J. Phys. Chem. A* **2008**, *112*, 1627–1632.

(22) Black, C. A.; Hanton, L. R.; Spicer, M. D. *Inorg. Chem.* **2007**, *46*, 3669–3679.

(23) Garau, C.; Quiñonero, D.; Frontera, A.; Ballester, P.; Costa, A.; Deyà, P. M. *J. Phys. Chem. A* **2005**, *109*, 9341–9345.

(24) (a) Fujita, M.; Tominaga, M.; Hori, A.; Therrien, B. *Acc. Chem. Res.* **2005**, *38*, 371–380. (b) Yoshizawa, M.; Kusukawa, T.; Kawano, M.; Ohhara, T.; Tanaka, I.; Kurihara, K.; Niimura, N.; Fujita, M. *J. Am. Chem. Soc.* **2005**, *127*, 2798–2799. (c) Tashiro, S.; Tominaga, M.; Kawano, M.; Therrien, B.; Ozeki, T.; Fujita, M. *J. Am. Chem. Soc.* **2005**, *127*, 4546–4547. (d) Takaoka, K.; Kawano, M.; Ozeki, T.; Fujita, M. *Chem. Commun.* **2006**, 1625–1627. (e) Yoshizawa, M.; Tamura, M.; Fujita, M. *Science* **2006**, *312*, 251–254. (f) Kawano, M.; Kobayashi, Y.; Ozeki, T.; Fujita, M. *J. Am. Chem. Soc.* **2006**, *128*, 6558–6559. (g) Nakabayashi, K.; Kawano, M.; Kato, T.; Furukawa, K.; Ohkoshi, S.; Hozumi, T.; Fujita, M. *Chem. Asian J.* **2007**, *2*, 164–170. (h) Yamaguchi, T.; Tashiro, S.; Tominaga, M.; Kawano, M.; Ozeki, T.; Fujita, M. *Chem. Asian J.* **2007**, *2*, 468–476. (i) Furusawa, T.; Kawano, M.; Fujita, M. *Angew. Chem., Int. Ed.* **2007**, *46*, 5717–5719. (j) Yamashita, K.; Kawano, M.; Fujita, M. *Chem. Commun.* **2007**, 4102–4103. (k) Nishioka, Y.; Yamaguchi, T.; Yoshizawa, M.; Fujita, M. *J. Am. Chem. Soc.* **2007**, *129*, 7000–7001. (l) Nakabayashi, K.; Ozaki, Y.; Kawano, M.; Fujita, M. *Angew. Chem., Int. Ed.* **2008**, *47*, 2046–2048. (m) Yamaguchi, T.; Fujita, M. *Angew. Chem., Int. Ed.* **2008**, *47*, 2067–2069. (n) Klosterman, J. K.; Iwamura, M.; Tahara, T.; Fujita, M. *J. Am. Chem. Soc.* **2009**, *131*, 9478–9479.

(25) (a) Schneider, B.; Cohen, D.; Berman, H. M. *Biopolymers* **1992**, *32*, 725–750. (b) Schneider, B.; Cohen, D. M.; Schleifer, L.; Srinivasan, A. R.; Olson, W. K.; Berman, H. M. *Biophys. J.* **1993**, *65*, 2291–2303. (c) Schneider, B.; Berman, H. M. *Biophys. J.* **1995**, *69*, 2661–2669. (d) Woda, J.; Schneider, B.; Patel, K.; Mistry, K.; Berman, H. M. *Biophys. J.* **1998**, *75*, 2170–2177. (e) Kabeláč, M.; Hobza, P. *Phys. Chem. Chem. Phys.* **2007**, *9*, 903–917.

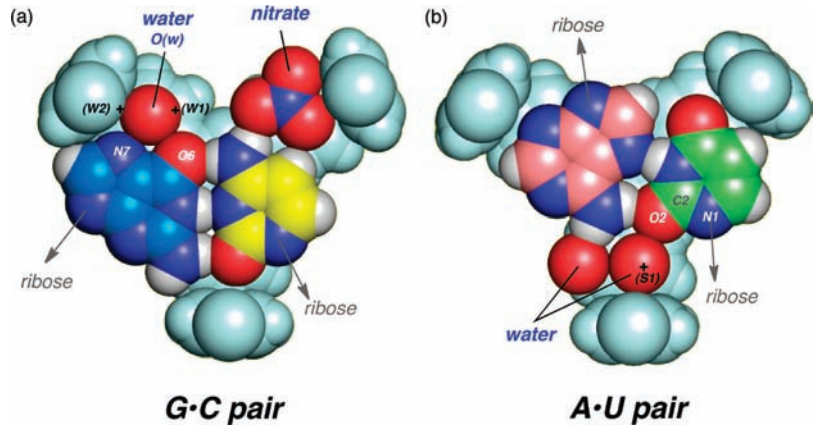

Figure 5. X-ray crystal structures showing the localized hydration and anion interactions for encapsulated single DNA base pairs. (a) **1′**⊃(**2b**·**3b**) and (b) **1′**⊃(**4**·**5**).[12] The top triazine panel and exterior solvent, counterions, and ribose phosphate groups have been removed for clarity.

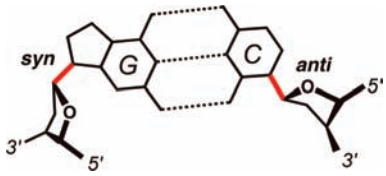

Figure 6. The *syn*, *anti*-ribose conformation of **1′**⊃(**2b**·**3b**).

precluded and two water molecules were instead coenclathrated (Figure 5b).[12] Because of the Hoogsteen conformation, the W2 position of adenine **4** is blocked by uridine **5** and the first water molecule is located close to the adenine W1 position. The second water molecule resides close to the S1 site of uridine **5** and is the furthest out of plane (N1−C2−O2−S1 torsion angle = 8°). The same two water molecules are also present for each A·U base pair in the dinucleotide monophosphate duplex crystal structure. To summarize, even within the hydrophobic cavity of cage **1** nucleobase pairs are hydrated at specific locations, similar to the hydration of base-pairs in DNA strands, and just like in DNA helices, the hydration sites are constrained by the local environment and neighboring molecules.

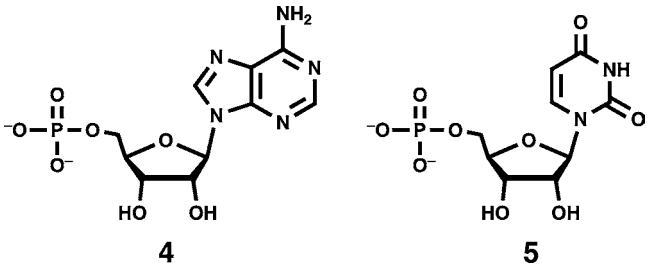

The ribose moieties of the enclathrated G·C pair assumed a syn-/anti-conformation more commonly observed in GC-rich Z-DNA duplex structures (Figure 6).[2a,26] The ribose unit of guanosine **2b** adopted the less common syn-conformation and formed a H-bond between the N3(G) and O5′(ribose) (N···(H)-O distance: 2.78 Å, Figure 3b). This H-bond stabilized the syn-conformation and no disordered ribose puckering was observed. Relative to the *N*-glycosidic bond, the ribose of cytidine **3b** adopted the regular anti-conformation, typical of standard B-DNA duplexes. No inter- or intramolecular H-bonds formed and the unrestrained ribose of **3b** was disordered between two sugar puckering modes (occupancy 38% and 62%, respectively; Figure S3.2 in Supporting Information).

Solution State Properties. In solution, the isolated Watson−Crick G·C base pair **1**⊃(**2a**·**3a**) retained remarkable selectivity and robustness, even in the absence of the templating DNA helix and stabilizing intra base-pair interactions. Independently, the three H-bonds in the Watson−Crick G·C base pair are weak (less than 20 kJ mol^{-1} each) but combine to generate one of the most robust H-bond motifs. Guanosine **2a** and cytidine **3a** present ADD and DAA hydrogen bonding groups, and when combined in a 1:1 ratio, only the Watson−Crick base pair was observed. However, both **2a** and **3a** can form homoleptic H-bond dimers,[27] and for comparison, homoleptic complexes were synthesized. In the absence of the complementary nucleoside partner, Job's plots revealed 2 equiv of **2a** or **3a** were encapsulated by cage **1** to give homoleptic complexes **1**⊃(**2a**)$_2$ and **1**⊃(**3a**)$_2$ (Figure 7a,b). The upfield shifts for the aromatic signals of **2a** and **3a** in the ^{1}H NMR spectra of the respective homoleptic complexes, **1**⊃(**2a**)$_2$ and **1**⊃(**3a**)$_2$, are similar to the shifts observed **1**⊃(**2a**·**3a**), but the signals of cage **1** were broadened only in **1**⊃(**2a**)$_2$ and remained sharp for **1**⊃(**3a**)$_2$ (Figure 8). The broadening of the cage signal for guanosine dimer **1**⊃(**2a**)$_2$ results from slow equilibrium processes (rotation, exchange, etc.) of **1**⊃(**2a**)$_2$ on the NMR time scale and indicates stronger host−guest interactions for the larger **2a**, stronger guest−guest interactions (i.e., hydrogen bonds), or both. The equilibrium processes of **1**⊃(**3a**)$_2$ are fast and the cage signals remain sharp. Hill plots of NMR titration experiments gave association constants (K_a) for **2a** and **3a** and confirmed the discrepancy in binding for **1**⊃(**2a**)$_2$ and **1**⊃(**3a**)$_2$; **2a**, $K_a = 1.2 \times 10^4$ [M^{-2}]; **3a**, $K_a = 1.0 \times 10^3$ [M^{-2}] (Figure 7c,d). Both Hill plots display a slight sigmoidal shape (Hill constant: **1**⊃(**2a**)$_2$ = 1.2, **1**⊃(**3a**)$_2$ = 1.1) indicating slight positive allosteric effects potentially arising from mismatched guest−guest H-bonds. The disparity in association constants, however, is better ascribed to host−guest interactions. Guanosine **2a** exhibits a larger aromatic surface than cytidine **2a** and thus is stronger bound through hydrophobic and aromatic−aromatic interactions. Aromatic−aromatic interactions between the electron rich guanine and the electron poor triazine panels of cage **1** gave

(26) (a) Wang, A. H.-J.; Quigley, G. J.; Kolpak, F. J.; Crawford, J. L.; van Boom, J. H.; van der Marel, G.; Rich, A. *Nature* **1979**, *282*, 680–686. (b) Wang, A. H.-J.; Quigley, G. J.; Kolpak, F. J.; van der Marel, G.; van Boom, J. H.; Rich, A. *Science* **1981**, *211*, 171–176. (c) Ho, P. S.; Moores, B. H. M. *Biopolymers* **1997**, *44*, 65–90.

(27) Takahashi, K.; Tachikawa, M. *J. Mol. Struct.: THEOCHEM* **2009**, *912*, 44–52.

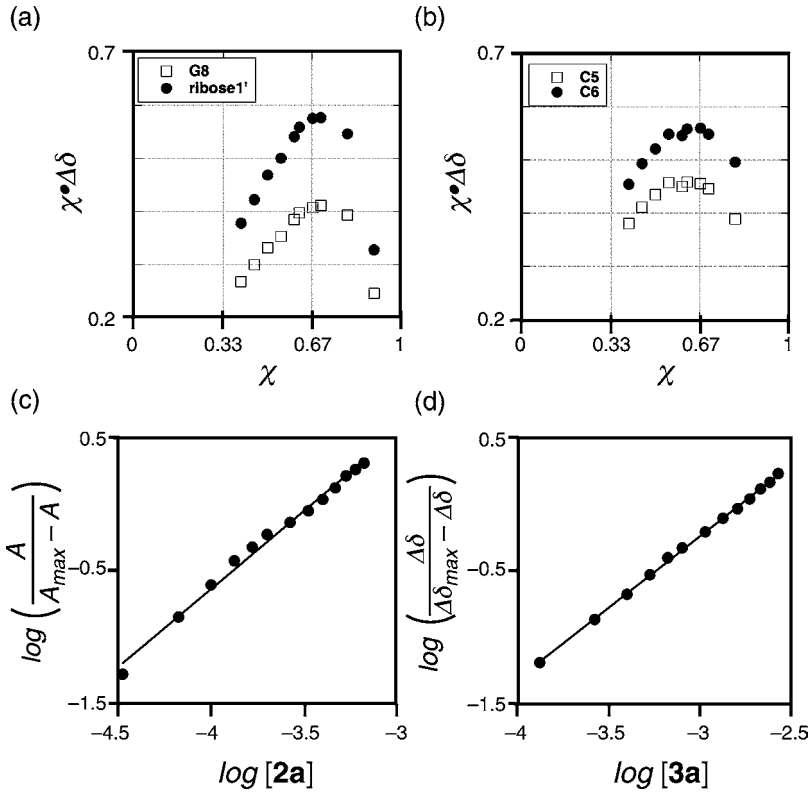

Figure 7. Binding of homoleptic nucleobase dimers by cage **1**. Job's plots reveal 1:2 H:G ratios for (a) **1**⊃(**2a**)$_2$ and (b) **1**⊃(**3a**)$_2$ and Hill plots from ^{1}H NMR titrations used to determine the association constants (K_a) for (c) **1**⊃(**2a**)$_2$ and (d) **1**⊃(**3a**)$_2$. (The titration was done at 295 K.)

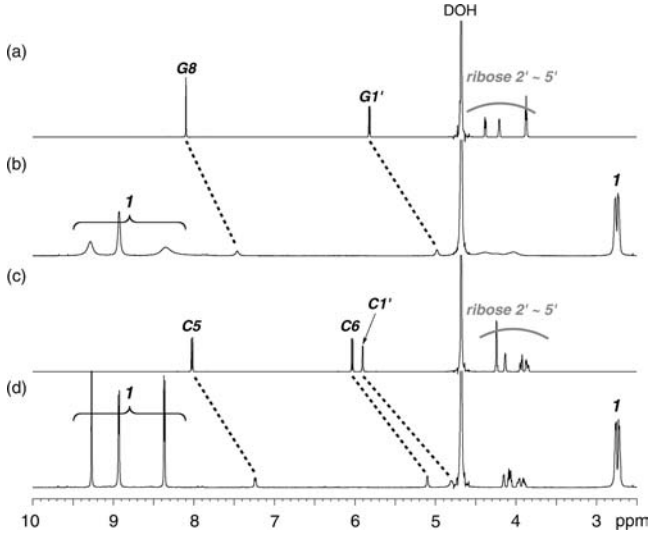

Figure 8. ^{1}H NMR spectra showing the formation of homoleptic base-pair host−guest complexes: (a) **2a**; (b) **1**⊃(**2a**)$_2$; (c) **3a**; and (d) **1**⊃(**3a**)$_2$ in D_2O.

rise to a host−guest charge transfer (CT) absorption band in the UV−vis spectra of **1**⊃(**2a**)$_2$ but not **1**⊃(**3a**)$_2$ (Figure 9).[28]

The intrinsic selectivity and stability of the triply bound single G·C pair was further examined using competition experiments. Mononucleotides uridine and adenine present an alternate doubly bound H-bond motif and can inhibit and compete with G·C base pair formation (Scheme 1). Sequential addition of competing mononucleotide to **1′**⊃(**2a**·**3a**) was monitored by ^{1}H NMR

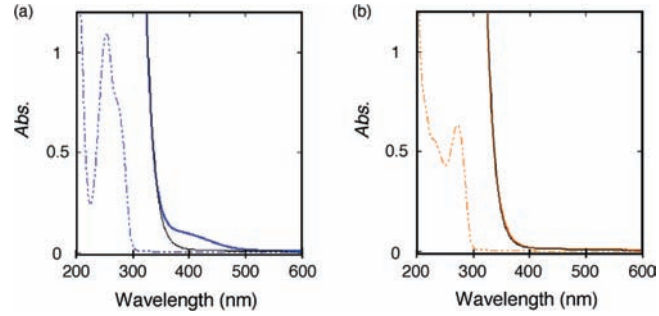

Figure 9. UV−vis spectra of encapsulated homoleptic nucleobase dimers (a) **1**⊃(**2a**)$_2$ and (b) **1**⊃(**3a**)$_2$ in H_2O, 1 mM, at room temperature. Empty cage **1** in solution is indicated as gray lines. Free mononucleotides in solution are shown as dashed lines.

spectroscopy and nucleobase G8, C5, and C6 signals shifted slightly downfield as the equivalents of inhibitor increased and equilibrium shifted to free **2a** or **3a** (Table 1). The ratio of encapsulated G·C base pair remaining was then estimated from the $\Delta\delta$. Upon addition of uridine **5**, the signals for cytidine **3a** shifted slightly downfield but signal G8 of **2a** was unaffected. The association constant of **2a** is 10 times larger than that for pyrimidine (**5**: $K_a = 1.2 \times 10^3$ [M^{-2}] at 22 °C) and the change in the NMR signals for **3a** indicates **5** competes with the less strongly bound **3a** and does not displace **2a**. However, the more stable Watson−Crick G·C base pair is favored, and even with 3 equiv of inhibitor **5**, approximately 70% of **1′**⊃(**2a**·**3a**) remained under equilibrium conditions (Figure 10a). Given that the mismatched G·U base pair differs only by a single H-bond, this moderate selectivity is quite impressive.

Similar to **2a**, purine 5′-adenosine monophosphate **4** has a stronger affinity for cage **1** ($K_a = 3.9 \times 10^3$ [M^{-2}] at 50 °C) and resulted in more pronounced downfield NMR shifts for both

(28) Such CT absorption bands between the host and guests were also discussed in previous reports. See references 13b,13d, and 13j.

Scheme 1. Representative Scheme Showing the Inhibition of G·C Base Pair **1**⊃(**2a**·**3a**) by H-Bond Competitor **5**

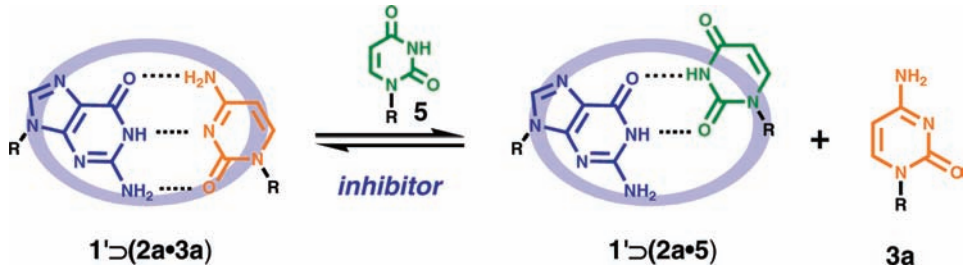

Table 1. $\Delta\delta^a$in ppm of G·C Base Pair Protons upon Addition of H-Bond Inhibitor i

	i = **5**			i = **4**		
χ_i	C5	C6	G8	C5	C6	G8
0.00	0.67	0.53	0.61	0.67	0.53	0.61
0.50	0.57	0.45	0.60	0.45	0.34	0.578
0.67	0.50	0.39	0.61	0.36	0.26	0.56
0.75	0.44	0.33	0.61	0.30	0.20	0.52

[a] Relative to the chemical shift of the free nucleobase proton in water.

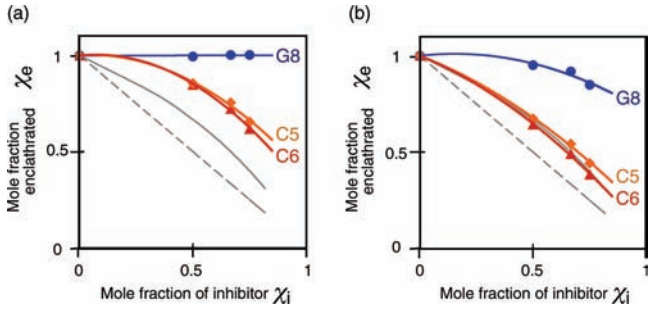

Figure 10. The mole fraction of encapsulated nucleobase remaining χ_e vs the mole fraction of added inhibitor, χ_i in case of (a) inhibitor **5** and (b) inhibitor **4**. χ_e was calculated from the δ/δ_o where δ_o is the initial chemical shift in **1**′⊃(**2a**·**3a**) and δ is the new equilibrium chemical shift upon addition of inhibitor i. The observed nucleobase protons are labeled. Solid gray lines simulate mole fractions in case of no selectivity between **2a** and **3a** nucleobases. Dashed gray lines simulate mole fractions of **3a** assuming **2a** remains 100% encapsulated. All spectra were measured at 323 K.

2a and **3a** when added to a solution of **1**′⊃(**2a**·**3a**). Cytidine **3a** was again primarily displaced, but adenosine **4** was also able to displace guanosine **2a**, but to a lesser extent. In spite of the stronger host−guest interactions for competitor **4**, the fidelity of the G·C base pair persisted and, at a 1:1:1 ratio of **2a**, **3a**, and **4**, the majority of the original G·C pairing (∼70%) remained (Figure 10b).

Electrostatic interactions with the highly cationic (12+) cage **1** can enhance the acidity of enclathrated guest molecules[13j] and a similar phenomena was predicted for the encapsulated guanosine N_1−H proton in **1**′⊃(**2a**·**3a**) and **1**′⊃(**2a**)$_2$. The generation of radicals and anions in DNA base pairs are thought to be important steps in DNA damage and are essential to understand the mechanisms of DNA damage.[29] Buried within the core of DNA and RNA helices, stacked nucleobases form an electronically coupled π-system and the pK_a values of acidic nucleobase protons (i.e., the N_1−H proton of guanosine) depend on the base pair sequence, proximity of phosphate anions, and the efficiency of the aromatic−aromatic interactions.[30] Upon the addition of base (aq. NaOH) the yellow solution of **1**′⊃(**2a**·**3a**) changed to orange with increasing pH due to stronger host−guest charge-transfer interactions with the deprotonated guanosine **2a** (Figure 11).[31] The isosbestic point at 410 nm revealed a one-to-one conversion and corroborated the removal of a single proton. From UV−vis titrations, the guanosine N_1−H pK_a was calculated to be 10.0 for base pair homodimer **1**′⊃(**2a**)$_2$ and 10.4 for the Watson−Crick base pair **1**′⊃(**2a**·**3a**). Within the cationic framework of host **1**′, the apparent guanosine pK_a has increased, but unlike free guanosine in water (pK_a 9.2−9.6),[32] **1**′⊃(**2a**·**3a**) and **1**′⊃(**2a**)$_2$ participate in H-bonds. An increase in guanosine acidity, via electrostatic interactions, should result in better hydrogen bond donation by the N_1−H and N_2−H_2 sites and a stronger base-pair.[33] Compared to the robust, triple H-bond motif of Watson−Crick base pair of **1**′⊃(**2a**·**3a**), the mismatched **1**′⊃(**2a**)$_2$ is stabilized to a lesser extent. In addition, host **1**′ protects and restricts access to the N_1−H proton and base-pair dissociation is a prerequisite for deprotonation.

Conclusion

In summary, we achieved the selective formation and recognition of a single Watson−Crick base pair in aqueous solution using a self-assembled coordination cage. The hydrophobic pocket of host **1** encapsulates and shields the individual base pairs from competing water solvent molecules. X-ray crystallography evinced the protected base pair and revealed multiple, interdependent host−guest and guest−guest interactions involving coencapsulated anions and water molecules. The specific anion−base pair interactions, localized hydration sites, and host−guest anion−π interactions are combined to arrange the various constituents to fully cover the large, planar host cavity. In addition, we demonstrated, using NMR competition

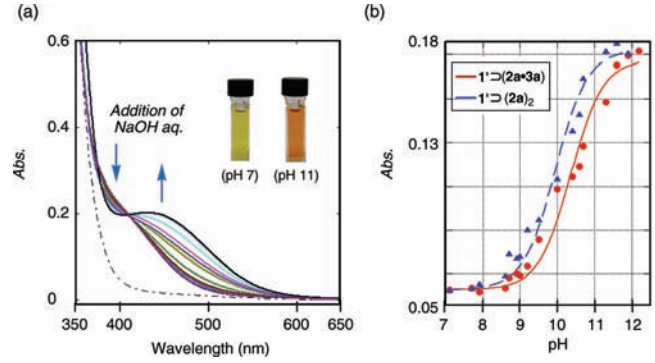

Figure 11. The pH titration of **1**′⊃(**2a**·**3a**) with aq NaOH (H_2O, 2.5 mM, room temperature). (a) The UV−vis spectra showing the change of CT absorption bands in various pH. Dashed line indicates the spectrum of **1**′. (b) The pH curve of **1**′⊃(**2a**·**3a**) is shown in red line and **1**′⊃(**2a**)$_2$ in blue line. Normalized by the concentration of **2a**.

(29) (a) Steenken, S. *Chem. Rev.* **1989**, *89*, 503–520. (b) Steenken, S. *Biol. Chem.* **1997**, *378*, 1293–1297. (c) Ghosh, A. K.; Schuster, G. B. *J. Am. Chem. Soc.* **2006**, *128*, 4172–4173.

experiments, that even a single Watson−Crick G·C base pair remains impressive selectivity over mismatched base pairs differing by only a single H-bond.

Experimental Section

Materials. Solvents and reagents were purchased from TCI Co., Ltd., WAKO Pure Chemical Industries Ltd., and Sigma-Aldrich Co. D_2O for NMR measurements and the reagents of ^{15}N labeled mononucleotide were purchased from Cambridge Isotope Laboratories, Inc. All chemicals were of reagent grades and used without any further purification. The cage **1** and **1′** was prepared according to the procedure described in previous report.[13a]

NMR Studies. All NMR spectral data were recorded on Bruker DRX 500 spectrometer or Bruker Avance 500 equipped with CP-TCI cryoprobe. These data were collected at ambient temperature unless otherwise noted.

X-ray Crystal Analysis of 1′⊃(2b·3b). The single crystal was obtained after the acetate buffer (pH 5.1) solutions of encapsulation complexes (20 mM) were slowly condensed at ambient temperature for a night. Data were collected on a Bruker APEX-II/CCD diffractometer equipped with a focusing mirror (MoKα radiation λ = 0.71073 Å) with a cryostat system equipped with a N_2 generator. The structures were solved by direct methods (SHELXS-97), and refined by full-matrix least-squares calculations on F^2 (SHELXL-97) by using the SHELX-TL program package. Hydrogen atoms were fixed at calculated positions and refined by using a riding model. The thermal temperature factors of solvents and nitrate ions were isotropically refined. On the basis of chemical geometry, several restraints were used for the ribose part of **3b** as well as nitrate ions because of severe disorder. $C_{103}H_{205}N_{46.5}O_{65.5}Pt_6$, M_r = 4280.15, crystal dimensions 0.06 × 0.06 × 0.03 mm^3, orthorhombic space group $P2_12_12$, a = 23. 601(4) Å, b = 25.572(5) Å, c = 27.944(5) Å, V = 16865(5) Å^3, Z = 4, ρ_{calcd} = 1.686 g cm^{-3}, F-(000) = 8505, radiation, λ(MoKα) = 0.71073 Å, T = 90(2) K, reflections collected/unique 195538/40025 (R_{int} = 0.0586). The structure was solved by direct methods (SHELXL-97) and refined by full-matrix least-squares methods on F^2 with 1918 parameters. R_1 = 0.0496 ($I > 2\sigma(I)$), wR_2 = 0.1293, GOF 1.075; max/min residual density 2.957/−2.146 eÅ^{-3}. (CCDC reference number 767546).

UV−Visible Absorption Measurements. UV−vis spectral data were recorded on a SHIMADZU UV-3150 using a quartz cell with 1 mm width at ambient temperature. The association constants (K_a) were estimated by titration experiments based on Hill equation.[34] In Hill plot, the maximum values of absorbance (A_{max}) or chemical shift ($\Delta\delta_{max}$) were calculated by a nonlinear curve-fitting procedure. In pK_a measurements, the basic solution of **1′**⊃(**2a·3a**) was prepared by addition of 0.1 N NaOH aqueous solution. The volume change by NaOH addition was less than 5% and negligibly small. The pH values of aqueous solution were measured by digital pH meter within the range of ±0.1 error. The pK_a values were estimated by pH titration based on Henderson−Hasselbalch equation.

Inhibition Experiments. The 0.1−0.3 mL aqueous solution of inhibitor **4** or **5** (20 mM) was added to the 0.5 mL solution of **1′**⊃(**2a·3a**) (4 mM) and then adjusted to total 1 mL D_2O solution. All ^1H NMR spectra were recorded at 323 K because of the severe signal broadening in equilibration at room temperature.

Acknowledgment. We thank Dr. Jeremy K. Klosterman for helpful discussions. T.S. thanks for a JSPS Research Fellowship for Young Scientists. This research was supported in part by Global COE Program (Chemistry Innovation through Cooperation of Science and Engineering), MEXT, Japan.

Supporting Information Available: Experimental details and spectroscopic data (PDF); data_sawa106 (CIF). This material is available free of charge via the Internet at http://pubs.acs.org.

JA101718C

(30) (a) Acharya, P.; Acharya, S.; Földesi, A.; Chattopadhyaya, J. *J. Am. Chem. Soc.* **2003**, *125*, 2094–2100. (b) Acharya, P.; Acharya, S.; Cheruku, P.; Amirkhanov, N. V.; Földesi, A.; Chattopadhyaya, J. *J. Am. Chem. Soc.* **2003**, *125*, 9948–9961. (c) Acharya, P.; Cheruku, P.; Chatterjee, S.; Acharya, S.; Chattopadhyaya, J. *J. Am. Chem. Soc.* **2004**, *126*, 2862–2869. (d) Chatterjee, S.; Pathmasiri, W.; Plashkevych, O.; Honcharenko, D.; Varghese, O. P.; Maiti, M.; Chattopadhyaya, J. *Org. Biomol. Chem.* **2006**, *4*, 1675–1686. (e) Kobayashi, K.; Yamagami, R.; Tagawa, S. *J. Phys. Chem. B* **2008**, *112*, 10752–10757.

(31) Such pH dependent changes of host−guest CT bands in cages were also discussed in previous reports. See reference 13j and Tashiro, S.; Fujita, M. *Bull. Chem. Soc. Jpn.* **2006**, *79*, 833–837.

(32) (a) Dawson, R. M. C. *Data for Biochemical Research*; Clarendon Press: Oxford, 1959. (b) Harris, T. K.; Turner, G. J. *IUBMB Life* **2002**, *53*, 85–98.

(33) This effect is limited as further acidification reduces the H-bond acceptor ability of O6. See (a) Sigel, R. K. O.; Freisinger, E.; Lippert, B. *J. Biol. Inorg. Chem.* **2000**, *5*, 287–299.

(34) Connors, K. A. *Binding Constants: The Measurement of Molecular Complex Stability*; Wiley: New York, 1987.